

Synthesis and Characterization of a Carbon Nanotube–Dendron Series for Efficient siRNA Delivery

M. Antonia Herrero,^{†,‡} Francesca M. Toma,^{†,§} Khuloud T. Al-Jamal,^{||}
Kostas Kostarelos,^{*,||} Alberto Bianco,^{*,⊥} Tatiana Da Ros,[†] Fouzia Bano,^{§,#}
Loredana Casalis,^{§,#} Giacinto Scoles,^{§,#} and Maurizio Prato^{*,†}

Center of Excellence for Nanostructured Materials, Department of Pharmaceutical Sciences, and INSTM, University of Trieste, Piazzale Europa 1, 34127 Trieste, Italy, Departamento de Química Orgánica, Facultad de Química, Universidad de Castilla-La Mancha, 13071 Ciudad Real, Spain, SISSA, 34014 Trieste, Italy, Nanomedicine Laboratory, Centre for Drug Delivery Research, The School of Pharmacy, University of London, London WC1N 1AX, U.K., CNRS, Institut de Biologie Moléculaire et Cellulaire, UPR9021 Immunologie et Chimie Thérapeutiques, 67000 Strasbourg, France, and Elettra, Synchrotron Laboratories, 34149 Trieste, Italy

Received May 4, 2009; E-mail: kostas.kostarelos@pharmacy.ac.uk; a.bianco@ibmc.u-strasbg.fr; prato@units.it

Abstract: A new series of dendron-functionalized multiwalled carbon nanotube (MWNT) derivatives, characterized by the presence of numerous positively charged tetraalkyl ammonium salts at the periphery of the dendron, has been synthesized. The positive charges on the MWNT surface, coupled with the unique ability of carbon nanotubes (CNTs) to penetrate cell membranes, make the new derivatives potentially ideal vectors for siRNA delivery. Using a fluorescently labeled, noncoding siRNA sequence, we demonstrate that cytoplasmic delivery of the nucleic acid is remarkably increased throughout the different dendron generations. The work reported here highlights the fact that dendron-functionalized CNTs can be rationally designed as efficient carriers of siRNA that can eventually lead to gene silencing.

Introduction

Biomedical applications of carbon nanotubes (CNTs) are currently the subject of intense investigations. Because of their unusual electrical and mechanical properties, CNTs can be considered innovative nanocarriers within the emerging platforms developed for therapeutic and diagnostic purposes in cancer nanotechnology.^{1,2} The possibility of exploiting a wide variety of methods for their functionalization with therapeutic molecules makes functionalized CNTs (*f*-CNTs) extremely attractive for novel drug development.³ Furthermore, the ability to penetrate into cells with remarkably reduced toxicity renders *f*-CNTs even more promising as

delivery systems.⁴ *f*-CNTs have been used to deliver anti-fungal and anticancer agents for the treatment of infectious diseases and cancer⁵ and have been modified with specific peptide-based ligands or antibodies to target malignant cells.⁶ *f*-CNTs have also been complexed with nucleic acids to

[†] University of Trieste.

[‡] Universidad de Castilla-La Mancha.

[§] SISSA.

^{||} University of London.

[⊥] CNRS.

[#] Elettra.

- (1) Peer, D.; Krap, J. M.; Hong, S.; Farokhzad, O. C.; Margalit, R.; Langer, R. *Nat. Nanotechnol.* **2007**, *2*, 751–760.
- (2) Bianco, A.; Kostarelos, K.; Prato, M. *Expert Opin. Drug Delivery* **2008**, *5*, 331–342.
- (3) (a) Bachilo, S. M.; Strano, M. S.; Kittrell, C.; Hauge, R. H.; Smalley, R. E.; Weisman, R. B. *Science* **2002**, *298*, 2361–2366. (b) Kam, N. W.; O'Connell, M.; Wisdom, J. A.; Dai, H. *Proc. Natl. Acad. Sci. U.S.A.* **2005**, *102*, 11600–11605. (c) Gannon, C. J.; Cherukuri, P.; Yakobson, B. I.; Cognet, L.; Kanzius, J. S. *Cancer* **2007**, *110*, 2654–2665. (d) Tasis, D.; Tagmatarchis, N.; Bianco, A.; Prato, M. *Chem. Rev.* **2006**, *106*, 1105–1136. (e) Prato, M.; Kostarelos, K.; Bianco, A. *Acc. Chem. Res.* **2008**, *41*, 60–68. (f) Chen, J.; Chen, S.; Zhao, X.; Kuznetsova, L. V.; Wong, S. S.; Ojima, I. *J. Am. Chem. Soc.* **2008**, *130*, 16778–16785.

- (4) (a) Kostarelos, K.; Lacerda, L.; Pastorin, G.; Wu, W.; Wieckowski, S.; Luangsivilay, J.; Godefroy, S.; Pantarotto, D.; Briand, J.-P.; Muller, S.; Prato, M.; Bianco, A. *Nat. Nanotechnol.* **2007**, *2*, 108–113. (b) Lacerda, L.; Bianco, A.; Prato, M.; Kostarelos, K. *Adv. Drug Delivery Rev.* **2006**, *58*, 1460–1470. (c) Boczkowski, J.; Lanone, S. *Nanomedicine* **2007**, *2*, 407–410. (d) Lacerda, L.; et al. *Adv. Mater.* **2008**, *20*, 225–230. (e) Kam, N. W. S.; Jessop, T. C.; Wender, P. A.; Dai, H. *J. Am. Chem. Soc.* **2004**, *126*, 6850–6851. (f) Lacerda, L.; Ali-Boucetta, H.; Herrero, M. A.; Pastorin, G.; Bianco, A.; Prato, M.; Kostarelos, K. *Nanomedicine* **2008**, *3*, 149–161. (g) Schipper, M. L.; Nakayama-Ratchford, N.; Davis, C. R.; Wong Shi Kam, N.; Chu, P.; Liu, Z.; Sun, X.; Dai, H.; Gambhir, S. S. *Nat. Nanotechnol.* **2008**, *3*, 216–221. (h) Singh, R.; Pantarotto, D.; Lacerda, L.; Pastorin, G.; Klumpp, C.; Prato, M.; Bianco, A.; Kostarelos, K. *Proc. Natl. Acad. Sci. U.S.A.* **2006**, *103*, 3357–3362. (i) Kostarelos, K. *Nat. Biotechnol.* **2008**, *26*, 774–776.
- (5) (a) Liu, Z.; Sun, X.; Nakayama-Ratchford, N.; Dai, H. *ACS Nano* **2007**, *1*, 50–56. (b) Ali-Boucetta, H.; Al-Jamal, K.; McCarthy, D.; Prato, M.; Bianco, A.; Kostarelos, K. *Chem. Commun.* **2008**, 459–461. (c) Feazell, R. P.; Nakayama-Ratchford, N.; Dai, H.; Lippard, S. J. *J. Am. Chem. Soc.* **2007**, *129*, 8438–8439. (d) Wu, W.; Wieckowski, S.; Pastorin, G.; Benincasa, M.; Klumpp, C.; Briand, J. P.; Gennaro, R.; Prato, M.; Bianco, A. *Angew. Chem., Int. Ed.* **2005**, *44*, 6358–6362.
- (6) (a) Liu, Z.; Cai, W.; He, L.; Nakayama, N.; Chen, K.; Sun, X.; Chen, X.; Dai, H. *Nat. Nanotechnol.* **2007**, *2*, 47–52. (b) McDevitt, M. R.; Chattopadhyay, D.; Kappel, B. J.; Jaggi, J. S.; Schiffman, S. R.; Antczak, C.; Njardarson, J. T.; Brentjens, R.; Scheinberg, D. A. *J. Nucl. Med.* **2007**, *48*, 1180–1189.

develop alternative gene transfer vector technologies against cancer and viral diseases.⁷

The delivery of small interference RNA (siRNA) using CNTs has previously been shown in cell culture^{7b,c,8} but is still little explored therapeutically. Knocking down expression of genes using siRNA is a promising approach for the treatment of a variety of disorders,⁹ but the efficacy of this therapeutic strategy is limited by the reduced capacity of siRNA to cross cell membranes and avoid protease degradation. Various transfection agents have been used to overcome these problems, but most often these vectors lead to serious cytotoxic side effects.¹⁰ Nonfunctionalized single-walled carbon nanotubes (SWNTs) coated with lipopolymers modified with siRNA were used to transfect human cells in order to silence the expression of HIV-specific cell surface receptors.^{7c} Alternatively, SWNTs covalently functionalized with small groups containing distal ammonium functions can also form electrostatic complexes with the negatively charged siRNA.^{7b,11}

In the most advanced study to date, we achieved therapeutic silencing using *f*-CNT-mediated delivery of a siRNA sequence leading to tumor-growth arrest and prolonged survival of animals bearing a human lung tumor xenograft.¹² Interestingly, that study included a comparison between the gene-silencing capacities of cationic CNTs (structure **1** in Scheme 1, which is protonated at physiological pH) and cationic liposomes. We found a statistically significant benefit from *in vivo* local (intratumoral) administration of siRNA:CNT complexes instead of siRNA:liposomes. The cationic nanotubes used were multiwalled carbon nanotubes (MWNTs) functionalized with ammonium groups at the periphery of a triethylene glycol chain introduced using the 1,3-dipolar cycloaddition reaction.¹³ This material dispersed well in water and allowed the formation of stable complexes with the phosphate ions of siRNA.¹² If the number of cationic functions at the surface of *f*-CNTs can be controllably increased, an opportunity to develop novel, highly soluble *f*-CNTs that can efficiently complex and deliver siRNA may become available.

On the basis of this hypothesis, we report in the present work the synthesis of successive generations of polyamidoamine (PAMAM) dendrons linked to the surface of MWNTs.¹⁴ The PAMAM dendrons attached to the MWNTs enhance their aqueous solubility through the presence of many polar groups. A stepwise synthetic process was followed to achieve growth of the dendrons on the MWNTs up to the second-generation. Pristine MWNTs, initially functionalized using 1,3-dipolar cycloaddition of azomethine ylides, were further modified by combining ethylenediamine and methyl acrylate in a divergent approach. The second-generation dendron bears the highest number of peripheral primary amino groups (four amino groups per dendron moiety), which eventually were subjected to a process of alkylation using an epoxy derivative.¹⁵ The same alkylation was also performed for each generation from G₀ to G₂. All of the dendron–MWNT generations were characterized by spectroscopic and microscopic techniques. The alkylated dendron–MWNT adducts were finally complexed with a noncoding siRNA sequence, and the complexes were successfully used to transfect mammalian cells. We discovered that the cytoplasmic delivery of siRNA remarkably increased in going from dendron generation G₀ to generation G₂ in comparison with the delivery by the precursor ammonium-functionalized MWNTs.

Results and Discussion

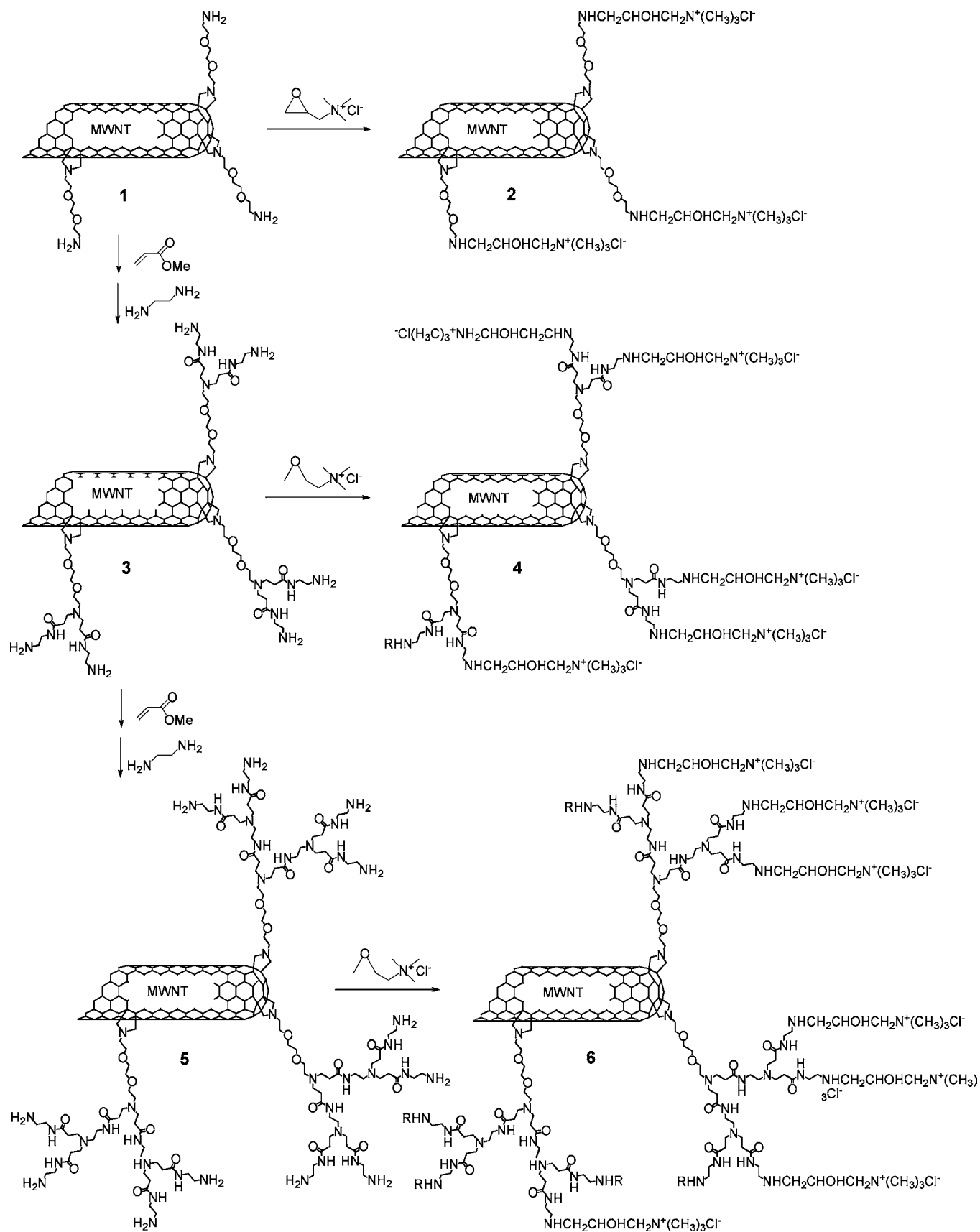
Design and Synthesis of Dendron–MWNTs.¹⁶ Functionalization of MWNTs using the 1,3-dipolar cycloaddition of azomethine ylides was used to introduce pyrrolidine moieties on the external surface and at the tips of MWNTs, forming the zeroth-generation (G₀) dendron–MWNT (**1** in Scheme 1). The first-generation (G₁) and second-generation (G₂) dendron–MWNTs **3** and **5**, respectively, were synthesized by repeating twice the two-step reaction using methyl acrylate and ethylenediamine. We proceeded to alkylate **1**, **3**, and **5** with a glycidyl trimethylammonium chloride epoxy derivative to generate the corresponding polycationic dendron–MWNTs **2**, **4**, and **6** (Scheme 1).¹⁵ The Kaiser test allowed quantification of the amino groups for the different generations of dendrons before alkylation.¹⁷ The test gave negative results for the alkylated conjugates **2**, **4**, and **6**, consistent with complete conversion of the primary amino groups. The amount of primary amino groups on **1** was measured by the Kaiser test as 481 μmol/g. Subsequent Kaiser tests gave amine loadings of 718 and 1097 μmol/g for the **3** and **5**, respectively.

The solubility of the charged dendron–MWNTs was assessed in water. The insets of Figure 1 display the differences in the dispersibility of the conjugates. A clear increase in solubility was observed going from the G₀ dendron–MWNT **1** to the more highly alkylated dendron generations. The aqueous solution of compound **6** was stable for at least 4 weeks at room temperature without formation of any precipitate, and a solubility of up to 3 mg/mL was obtained.

Characterization of Dendron–MWNTs. The different *f*-CNT conjugates were fully characterized by standard techniques,

- (7) (a) Pantarotto, D.; Singh, R.; McCarthy, D.; Erhardt, M.; Briand, J.-P.; Prato, M.; Kostarelos, K.; Bianco, A. *Angew. Chem., Int. Ed.* **2004**, *43*, 5242–5246. (b) Zhang, Z.; Yang, X.; Zhang, Y.; Zeng, B.; Wang, S.; Zhu, T.; Roden, R. B. S.; Chen, Y.; Yang, R. *Clin. Cancer Res.* **2006**, *12*, 4933–4939. (c) Liu, Z.; Winters, M.; Holodniy, M.; Dai, H. *Angew. Chem., Int. Ed.* **2007**, *46*, 2023–2027. (d) Lacerda, L.; Bianco, A.; Prato, M.; Kostarelos, K. *J. Mater. Chem.* **2008**, *18*, 17–22. (e) Liu, Y.; Wu, D. C.; Zhang, W. D.; Jiang, X.; He, C. B.; Chung, T. S.; Goh, S. H.; Leong, K. W. *Angew. Chem., Int. Ed.* **2005**, *44*, 4782–4785. (f) Lu, Q.; Moore, J. M.; Huang, G.; Mount, A. S.; Rao, A. M.; Larcom, L. L.; Ke, P. C. *Nano Lett.* **2004**, *4*, 2473–2477. (g) Gao, L.; Nie, L.; Wang, T.; Qin, Y.; Guo, Z.; Yang, D.; Yan, X. *ChemBioChem* **2006**, *7*, 239–242.
- (8) (a) Kam, N. W. S.; Liu, Z.; Dai, H. *J. Am. Chem. Soc.* **2005**, *127*, 12492–12493. (b) Lanner, J. T.; Bruton, J. D.; Assefaw-Redda, Y.; Andronache, Z.; Zhang, S.-J.; Severa, D.; Zhang, Z.-B.; Melzer, W.; Zhang, S.-L.; Katz, A.; Westerblad, H. *FASEB J.* **2009**, *23*, 1728–1738.
- (9) Dykxhoorn, D. M.; Lieberman, J. *Cell* **2006**, *126*, 231–235.
- (10) Nguyen, T.; Menocal, E. M.; Harborth, J.; Fruehauf, J. H. *Curr. Opin. Mol. Ther.* **2008**, *10*, 158–167.
- (11) (a) Krajcik, R.; Jung, A.; Hirsch, A.; Neuhuber, W.; Zolk, O. *Biochem. Biophys. Res. Commun.* **2008**, *369*, 595–602. (b) Wang, X.; Ren, J.; Qu, X. *ChemMedChem* **2008**, *3*, 940–945.
- (12) Podesta, J. E.; Al-Jamal, K. T.; Herrero, M. A.; Tian, B.; Ali-Boucetta, H.; Hegde, V.; Bianco, A.; Prato, M.; Kostarelos, K. *Small* **2009**, *5*, 1176–1185.
- (13) (a) Georgakilas, V.; Kordatos, K.; Prato, M.; Guldi, D. M.; Holzinger, M.; Hirsch, A. *J. Am. Chem. Soc.* **2002**, *124*, 760–761. (b) Georgakilas, V.; Tagmatarchis, N.; Pantarotto, D.; Bianco, A.; Briand, J.-P.; Prato, M. *Chem. Commun.* **2002**, 3050–3051.

- (14) Campidelli, S.; Soombar, C.; Diz, E. L.; Ehli, C.; Guldi, D. M.; Prato, M. *J. Am. Chem. Soc.* **2006**, *128*, 12544–12552.
- (15) Oh, S.-K.; Kim, Y.-G.; Ye, H.; Crooks, R. M. *Langmuir* **2003**, *19*, 10420–10425.
- (16) Tomalia, D. A.; Baker, H.; Dewald, J. R.; Hall, M.; Kallos, G.; Martin, S.; Roeck, J.; Ryder, J.; Smith, P. *Polym. J.* **1985**, *17*, 117–132.
- (17) Sarin, V. K.; Kent, S. B. H.; Tam, J. P.; Merrefield, R. B. *Anal. Biochem.* **1981**, *117*, 147–157.

Scheme 1. Synthesis of Dendron–MWNTs^a

^a Reaction conditions for alkylation of primary amino groups with glycidyl trimethylammonium chloride: MeOH, 40 °C, 48 h. R = $\text{CH}_2\text{CHOHCH}_2\text{N}^+(\text{CH}_3)_3\text{Cl}^-$.

including thermogravimetric analysis (TGA), transmission electron microscopy (TEM), and atomic force microscopy (AFM).

The amount of functional groups in the *f*-MWNTs was quantified by TGA. The weight loss for the highly functionalized

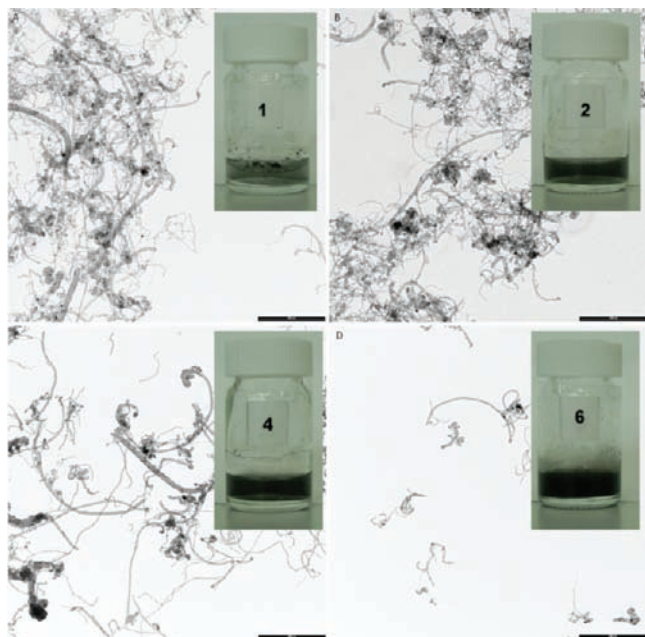


Figure 1. TEM images of (A) G_0 dendron-MWNT **1**, (B) alkylated G_0 dendron-MWNT **2**, (C) alkylated G_1 dendron-MWNT **4**, and (D) alkylated G_2 dendron-MWNT **6**. The scale bar is 1 μm . The corresponding insets show images of solutions of **1**, **2**, **4**, and **6** (all solubilized at 1 mg/mL in H_2O).

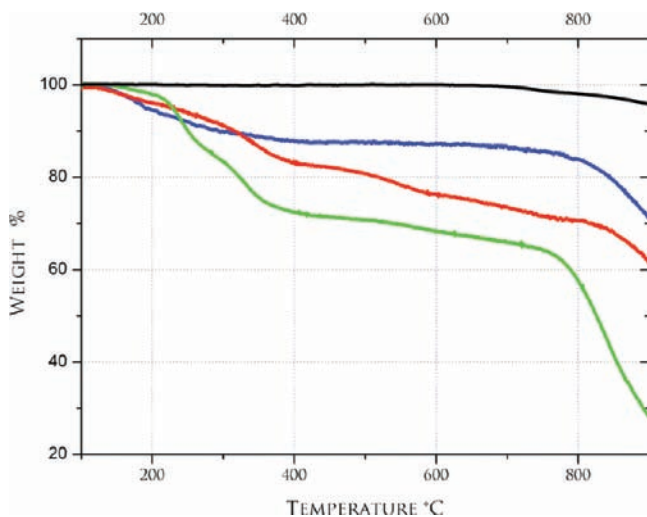


Figure 2. TGA curves for pristine MWNTs (black line), G_1 dendron-MWNTs **3** (blue line), G_2 dendron-MWNTs **5** (red line), and alkylated G_2 dendron-MWNTs **6** (green line). All of the experiments were performed under a N_2 atmosphere.

conjugates, as calculated from the thermogravimetric curves at 450 $^\circ\text{C}$, was directly correlated to the increase of mass around the CNTs introduced at each step. The mass attributed to functionalities increased from 12.5% in the first-generation dendron-MWNT **3** to 18% in the second-generation dendron-MWNT **5**. The final derivative **6** showed a 28% mass loss (Figure 2). The amount of the functional groups for the final dendron-MWNT **6** calculated from the TGA curve was 237 $\mu\text{mol/g}$, corresponding to 948 $\mu\text{mol/g}$ of amine groups for the precursor G_2 dendron-MWNT **5**. This value was in good agreement with the value found using the Kaiser test (1097 $\mu\text{mol/g}$).

The functionalized MWNTs were further structurally studied by TEM (Figure 1). The images confirmed the presence of

MWNTs and showed morphological differences for the different dendron generations in water, including a remarkable increase in the degree of dispersibility. In addition to TEM, alkylated G_2 dendron-MWNT **6** was characterized by AFM, which was performed by depositing a sample of the aqueous dispersion on a mica surface. A progressive increase in the diameter of the nanotubes as the dendritic structure grew was observed. The AFM images showed individual MWNTs as well as small bundles present in the sample. Three-dimensional (3D) views of cropped sections of Boc-amino-protected MWNT **1** and dendron-MWNT **6** from $1.2 \times 1.2 \mu\text{m}^2$ AFM topographic images, along with their line profiles, are shown in Figure 3A, B. A clear increase in the diameter of the MWNT conjugates for the later dendron generations can be seen. To evaluate the average profile, the diameters of pristine MWNTs, Boc-amino-protected MWNTs **1**, and dendron-MWNTs **6** were measured, and values ranging from 21–25 nm for **1** and up to 36–40 nm for **6** were obtained (Figure 3C).

Effect of the Different Dendron Generations on Cellular Uptake of Alkylated Dendron-MWNT:siRNA Complexes. To establish if complexation of the different generations of the alkylated dendron-MWNTs with siRNA had any effect on the degree of cellular uptake of siRNA, human cervical carcinoma (HeLa) cells were incubated with the dendron-MWNTs complexed with a noncoding siRNA sequence. In order to observe whether the siRNA was internalized in cells, it was fluorescently labeled at the 3' end with Atto 655, which emits light in the far-red region ($\lambda_{\text{em}} = 690 \text{ nm}$). The fluorescently labeled siRNA was complexed with each conjugate of the synthesized dendron-MWNT series at a 1:16 mass ratio as previously optimized,¹² and cellular uptake was observed using confocal microscopy under identical optical conditions.

Figure 4 shows that the dendron-MWNTs with increased degrees of branching exhibited more effective intracellular siRNA delivery than did MWNTs **1** and alkylated dendron-MWNTs **2**, while almost no uptake of siRNA alone was observed (Figure 4a). Both the siRNA (the blue channel in Figure 4) and the f -MWNTs [the differential interference contrast (DIC) images in Figure 4] were internalized within the cell cytoplasm, but it is not yet clear whether the siRNA was detached from the f -MWNTs intracellularly. The fluorescent signal from the Atto 655-labeled siRNA was found to be diffused throughout the cytoplasm of cells treated with the dendron-MWNT:siRNA complexes, without any indication of localization in intracellular vesicles (usually evidenced by highly fluorescent pockets within the cell). The morphology of the cells did not seem to be affected by the dendron-MWNTs throughout these studies, indicating that the uptake of siRNA was not a result of cellular damage but presumably due to translocation of the dendron-MWNTs through the plasma membrane. Confocal microscopy studies at earlier time points (4 h) after incubation of the f -MWNT:siRNA complexes indicated fluorescence signals of lower intensity in comparison with the 24 h data shown here. At both time points, the fluorescent signal from the Atto 655-labeled siRNA was observed throughout the cell volume without localization in the nucleus or other cellular compartment. However, the cellular internalization of the siRNA was always nanotube-dependent. In order to gain a better understanding of the mechanism by which dendritic and ammonium-functionalized MWNT:siRNA complexes enter and are transported within cells, systematic cell-trafficking studies of these complexes are warranted and currently under investigation in our laboratories. This data shows that higher dendron

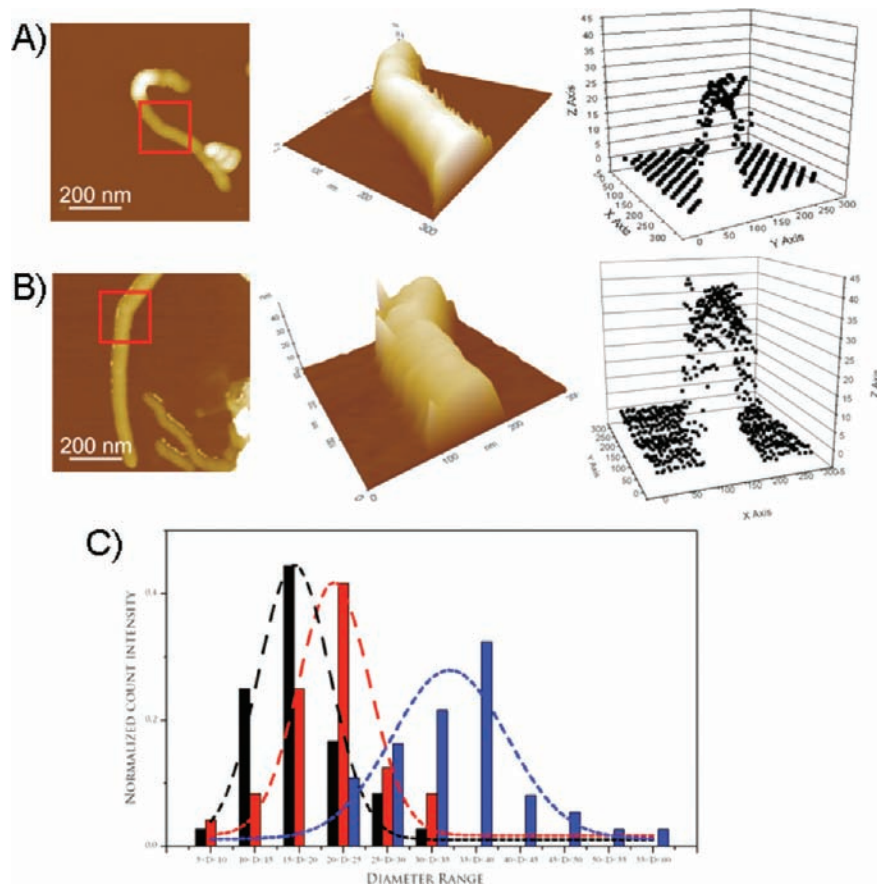


Figure 3. (A, B) (left) AFM topographic images ($1.2 \times 1.2 \mu\text{m}^2$) of (A) MWNTs after the 1,3-dipolar cycloaddition reaction (Boc-amino-protected MWNTs **1**) and (B) alkylated G₂ dendron-MWNTs **6**, along with (center) 3D views of cropped segments [corresponding to the red square boxes in (A) and (B)] and (right) line profiles. (C) Diameter distributions of pristine MWNTs (black), **1** (red), and **6** (blue). The three curves represent Gaussian fits of the data.

generations grown on the MWNT surface could lead to more efficient cytoplasmic delivery of siRNA, indicating that such constructs can potentially lead to highly effective levels of gene silencing.

Conclusions

In summary, we have described the synthesis, characterization, and cell uptake of a series of different-generation alkylated dendron-MWNT derivatives. Dendron synthesis on the MWNT surface was performed using the divergent methodology followed by step involving alkylation of the peripheral primary amino groups of the different dendrons. The new dendron-MWNT constructs were characterized by standard analytical techniques, including TGA, TEM, and AFM. The polycationic properties of the dendron coupled with the unique capacity of CNTs to penetrate cell membranes make the new derivatives potentially ideal vectors for siRNA delivery. Using a fluorescently labeled, noncoding siRNA sequence, we have shown that internalization of the alkylated dendron-MWNT:siRNA complexes was improved for the later dendron generations. Further studies to elucidate the mechanism of cellular internalization and intracellular trafficking of the dendron-MWNT:siRNA complexes are warranted. The work reported here demonstrates that with respect to the single-chain derivative **1**, dendron-functionalized CNTs are much more efficient carriers of siRNA for the development of novel gene silencing and knockdown therapies. This result, coupled with the better behavior of **1** than liposomes in transporting siRNA, make the new dendron-based

derivatives very promising substrates for applications in nanomedicine.

Experimental Section

Materials. MWNTs (stock no. 1240XH, 95%, o.d. 20–30 nm) were purchased from Nanostructured & Amorphous Materials, Inc. Chemicals and solvents for synthesis were obtained from Sigma-Aldrich and used as received. To achieve the synthesis of *f*-CNTs **1**, **3**, and **5**, we followed the procedure reported in refs 13, 14, and 18. Noncoding siRNA was obtained from Eurogentec. Minimum essential medium (MEM), fetal bovine serum (FBS), penicillin/streptomycin, and phosphate buffered saline (PBS) were purchased from Gibco, Invitrogen, and the cervical cancer cell line HeLa (CCL-2.2) was obtained from ATCC.

Characterization Techniques. TGA was performed under N₂ using a TGA Q500 analyzer (TA Instruments) by equilibrating at 100 °C and then following a ramp of 10 °C/min up to 900 °C. TEM analyses were performed on a Philips EM208 transmission electron microscope using an accelerating voltage of 100 kV; 0.2 mg of each dendron-MWNT generation was dispersed in 1 mL of water, and 1 drop of this solution was deposited on a TEM grid (200 mesh, Nichel, carbon only or carbon lacey). AFM samples were prepared by the deposition of 1 drop of a highly diluted nanotube solution onto a mica substrate and spin-coating in a row. Boc-amino-protected MWNTs **1** after cycloaddition were dispersed in DMF and dendron-MWNTs **5** and alkylated dendron-MWNTs **6** in MeOH. The samples were examined with an XE-series

(18) Kordatos, K.; Da Ros, T.; Bosi, S.; Vazquez, E.; Bergamin, M.; Cusan, C.; Pellarini, F.; Tomberli, V.; Baiti, B.; Pantarotto, D.; Georgakilas, V.; Spalluto, G.; Prato, M. *J. Org. Chem.* **2001**, *66*, 4915–4920.

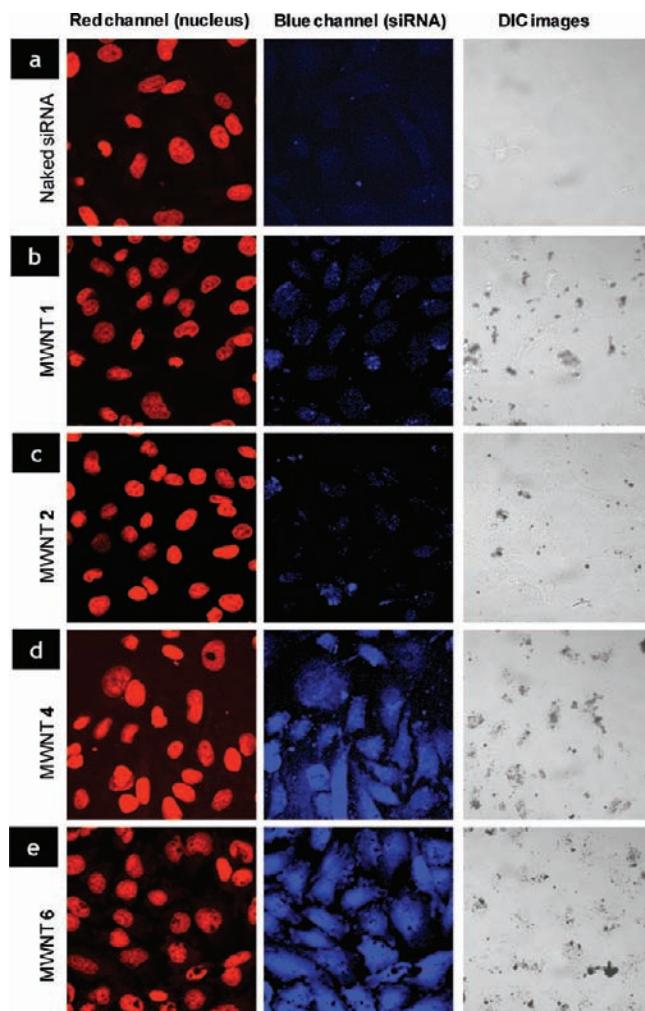


Figure 4. Confocal microscopy images of HeLa cells obtained after 24 h of incubation with (a) Atto 655-labeled siRNA alone and with Atto 655-labeled siRNA complexed to (b) G₀ dendron–MWNTs **1**, (c) alkylated G₀ dendron–MWNTs **2**, (d) alkylated G₁ dendron–MWNTs **4**, and (e) alkylated G₂ dendron–MWNTs **6** at a 1:16 mass ratio and siRNA concentration of 80 nM (equivalent to 16 $\mu\text{g}/\text{mL}$ dendron–MWNTs). Cells were incubated with the complexes for 4 h in serum-free medium, after which serum was added to reach a final serum concentration of 10%. Nuclei were counterstained with propidium iodide. The images display an increase in the intracellular uptake of siRNA, as shown by the increase in the blue fluorescence of siRNA, in the following order: (e) > (d) > (c) > (b). siRNA alone (a) gave almost no detectable fluorescence in the cells.

microscope [Park Scientific Instruments Advanced Corp. (PSIA)] at room temperature. In all of the AFM measurements, the images were taken in noncontact (NC) mode with scan speed of 0.3 Hz using standard silicon rectangular cantilevers (PSIA, 950M-ACTA) with nominal spring constants of 40 N/m and radius of curvature <10 nm. In the NC-AFM measurements, the tip was scanned over the sample with a drive frequency of 330 kHz to acquire topographic images of various sizes (1.2–5 μm). The distributions of average diameters were obtained by estimating the diameters of single MWNTs (with and without functionalizations) from NC-AFM topographic images and their corresponding average line profiles. To evaluate the distribution of average diameters, 36, 24, and 37 nanotubes were observed for pristine MWNTs, **1**, and **6**, respectively.

Synthesis of Alkylated G₀ Dendron–MWNTs (2**).** A 10 mg sample of MWNTs **1** was added to 5 mg of glycidyl trimethylammonium chloride in 15 mL of MeOH, and the resulting mixture was kept at 40 °C for 2 days. The dendron–MWNT product **2** was filtered with a Millipore system (JH 0.45 μm filter), sonicated

for 30 min in MeOH, and then filtered and sonicated again. Following a final filtration, alkylated G₀ dendron–MWNTs **2** were obtained as a fine black powder (10 mg).

Synthesis of Alkylated G₁ Dendron–MWNTs (4**).** A 10 mg sample of MWNTs **3** was added to 7.6 mg of glycidyl trimethylammonium chloride in 15 mL of MeOH, and the resulting mixture was kept at 40 °C for 2 days. The dendron–MWNT product **4** was filtered with a Millipore system (JH 0.45 μm filter), sonicated for 30 min in MeOH, and then filtered and sonicated again. Following a final filtration, alkylated G₁ dendron–MWNTs **4** were obtained as a fine black powder (10 mg).

Synthesis of Alkylated G₂ Dendron–MWNT (6**).** A 70 mg sample of MWNTs **5** was added to 755 mg of glycidyl trimethylammonium chloride in 70 mL of MeOH, and the resulting mixture was kept at 40 °C for 2 days. The dendron–MWNT product **6** was filtered with a Millipore system (JH 0.45 μm filter), sonicated for 30 min in MeOH, and then filtered and sonicated again. Following a final filtration, alkylated G₂ dendron–MWNTs **6** were obtained as a fine black powder (72 mg).

Evaluation of Fluorescent siRNA Complex Uptake in HeLa Cells. Atto 655-labeled siRNA ($\lambda_{\text{ex}} = 665 \text{ nm}$, $\lambda_{\text{em}} = 690 \text{ nm}$) was used to prepare fluorescent siRNA complexes. siRNA was complexed with the different generations of dendron–MWNTs at a 1:16 mass ratio. HeLa cells were grown to confluency on glass coverslips in 24-well tissue culture dishes (Corning B.V.) at a density of 50 000 cells per well in MEM supplemented with 10% FBS and 1% penicillin/streptomycin. After 24 h, the cells were transfected with noncoding siRNA conjugated to Atto 655. Briefly, 50 μL of the preformed siRNA complex was diluted 10 times with complete medium, and 500 μL of the complex-containing medium was added to each well, yielding a final siRNA concentration of 80 nM (1 $\mu\text{g}/\text{mL}$). The cells were incubated with the *f*-MWNT:siRNA complexes for 4 h in serum-free medium, after which serum was added to achieve a final serum concentration of 10%. After 24 h, the cells were washed with PBS solution, fixed with 4% paraformaldehyde (Sigma) in PBS for 15 min at room temperature, and then rinsed with PBS. For nuclear staining, cells were permeabilized with 0.1% Triton X-100 in PBS for 10 min at room temperature, treated with RNAase (100 $\mu\text{g}/\text{mL}$) (Sigma) for 20 min at 37 °C, incubated with 1 mg/mL propidium iodide (Molecular Probes) in PBS for 5 min, and then rinsed three times with PBS. Coverslips were mounted with aqueous poly(vinyl alcohol) Citifluor reagent mixed with AF100 antifade reagent (10:1) (Citifluor) prior to use. Slides were examined under the CLSM using a 63 \times oil immersion lens.

Acknowledgment. This work was supported by the University of Trieste, INSTM, Italian Ministry of Education MUR (cofin Prot. 2006034372 and Fibr RBIN04HC3S), Regione Friuli Venezia-Giulia, SISSA Trieste, The School of Pharmacy, University of London, the CNRS, and the Agence Nationale de la Recherche (Grant ANR-05-JCJC-0031-01). Partial support by the European Union FP6 NEURONANO (NMP4-CT-2006-031847), NINIVE (NMP4-CT-2006-033378), and FP7 ANTICARB (HEALTH-2007-201587) Programs is also acknowledged. The Elettra group acknowledges partial financial support from IIT (Italian Institute of Technology) and CBM (Consortium for Molecular Biomedicine). M.A.H. acknowledges support by the Junta de Comunidades de Castilla la Mancha (Spain) through the award of a postdoctoral fellowship.

Supporting Information Available: Additional characterization data for all compounds, including TEM and TGA results, and complete ref 4d. This material is available free of charge via the Internet at <http://pubs.acs.org>.

JA903316Z